Appendix

This appendix describes the mathematical model that generated the results reported in the main text. The mathematical models for detection and congestion are given in §A and §B, respectively. The costs are quantified in §C and the strategy optimization and evaluation are defined in §D. Alternative modes of testing are discussed in §E, a radiological source is considered in §F, and supplementary computational results appear in §G.

A Detection Modeling

This section contains mathematical models for three detection processes: passive neutron detection in §A.1, passive gamma-ray detection in §A.2, and radiography in §A.3. All parameter values related to the detection process are given in Table 1. For all three tests, these models are used in §A.4 and §A.5 to compute the false positive probabilities and detection probabilities, respectively.

A.1 Passive Neutron Detection

Emissions emanate from three sources: the weapon, the contents of a typical container that contains no weapons, and the background level in the absence of containers. The monitor is placed $r = 2$ m from the center of the container, which passes through the portal at velocity $v = 2.22$ m/sec (i.e., 5 mph). Hence, if we denote the container length by L, it takes $L/v = 5.5$ sec to monitor a 40-ft (or 12.2-m) container and 2.75 sec to monitor a 20-ft container. After t time units of detection, the true (i.e., ignoring measurement noise) cumulative emissions at the detector due to a stationary source with emission rate S_N that is a distance r from the detector is $\frac{A\epsilon_N S_N t}{4\pi r^2}$ [1], where A is the area of the radiation detector, and ϵ_N is the efficiency for detecting neutrons. Because our source is moving, the true cumulative emissions at the detector will be, for $L = 20$ or 40 ft,

$$\frac{A\epsilon_N S_N}{4\pi} \int_0^{L/v} \frac{dt}{r^2 + (vt - \frac{L}{2})^2} = \frac{\tan^{-1}\left(\frac{L}{2r}\right) A\epsilon_N S_N}{2\pi v r}, \tag{1}$$

if we assume that the weapon is placed in the middle of the container.

We assume that the true cumulative (sea-level terrestrial) background emissions after L/v time units is a normal random variable B_N with mean $A\epsilon_N b_N L/v$ and standard deviation $\sqrt{A\epsilon_N b_N L/v}$ (in units of neutrons) [1], where b_N is the mean neutron background rate.

After L/v time units of detection, we assume that a typical container (containing no weapons) has cumulative emissions at the detector equal to $\frac{A\epsilon_N C_N L}{4\pi r^2 v}$, where C_N is a log-normal random variable (i.e., it varies from container to container) with median e^{c_N} and dispersion factor $e^{\sigma_{cN}}$.

Finally, we incorporate measurement noise by assuming that all measurements are normal random variables (denoted by X_N), where the standard deviation is the unknown factor k_N times the square root of the mean. This relationship holds for a Poisson random variable, and is consistent with the observation that measurement errors typically grow with the magnitude of the measurement. Because the means themselves are random variables due to variation in the container contents and background, X_N will actually be a mixture of normals.

Parameter values for A, ϵ_N and b_N are taken from [1]. To estimate the noise factor k_N, we note that when the detection time is $t = 10$ sec, $r = 2$ meters and $S_N = 20$k neutrons/sec, the false positive probability and false negative probability from extensive controlled experiments (with stationary sources and in the absence of containers and background variation) were 10^{-4} and 10^{-3}, respectively [2]. Substituting these values into

$$P\Big(X_{N1} > s_N\Big) = 10^{-4}, \tag{2}$$

$$P\Big(X_{N2} < s_N\Big) = 10^{-3}, \tag{3}$$

where X_{N1} and X_{N2} are normally distributed with standard deviation equal to k_N times the square root of the mean, and where the means are $A\epsilon_N b_N t$ and $\frac{A\epsilon_N S_N t}{4\pi r^2} + A\epsilon_N b_N t$, respectively, and solving for the two unknowns (the test's threshold level s_N in [2] and the noise factor k_N) yields the value of k_N in Table 1. Finally, we set $c = -\infty$, $\sigma_c = 0$ (i.e., the random variable C_N is always zero) because 163k roadside field tests for container trucks resulted in no alarms [2].

A.2 Passive Gamma-ray Detection

The modeling of passive gamma-ray detection is similar to that of passive neutron detection. We retain the same notation, but use the subscript G in place of N; the values of A, r and v are the same for both types of passive detection. In contrast to passive neutron testing, the remaining parameters for passive gamma testing depend on whether the weapon contains plutonium or uranium. We derive the remaining parameter values for the plutonium weapon first, and then discuss the uranium weapon. While gamma rays are emitted at a variety of energies, we focus on the 0.662-MeV gamma ray in the case of passive radiation, which is the most prominent emission from the plutonium weapon in the main text [1]. The values b_G =1400 gamma rays/m^2·sec and $\epsilon_G = 0.70$ are taken from [1]. The noise factor k_G is estimated from vendor information, stating that the false positive probability is 10^{-3} and 10 grams of ^{239}Pu can be detected with probability 0.5 by a portal monitor with a pillar spacing of 20 ft ($r = 3$ m) at a passage speed of 5 mph in a 20μR/hr background [4]. To find the source term S_G for this experiment, we note that the 0.662 MeV emissions from weapons-grade plutonium are due to a decay product of ^{241}Pu [1] with decay rate 174,000/g·sec [5]. Because 0.44% of weapons-grade plutonium is made up of ^{241}Pu [1], we have $S_G = 0.0044(10)(174,000) = 7656$ gamma rays/sec. To find the background term b_G (we assume the background noise in this experiment is zero), we calculate that 4.53% of the energy from background radiation is at 0.662MeV [6] assuming a 10% energy resolution [1], so that the background radiation should contain 0.0091 μSv/hr at 0.662MeV. Using the conversion factor of 1.0 μSv/hr = 8.94$\times 10^5$ gamma rays/m^2·sec in a NaI detector at 0.662 MeV [7, 8], we find that the background radiation is 7656 gamma rays/m^2·sec at 0.662 MeV. Substituting $S_G = 7656$ gamma rays/sec, $b_G = 7656$ gamma rays/m^2·sec (the two 7656's are coincidental), $r = 3$ m and $L =$ 40 ft into

$$P\Big(X_{G1} > s_G\Big) = 10^{-3}, \tag{4}$$

$$P\Big(X_{G2} < s_G\Big) = 0.5, \tag{5}$$

where, for $i = 1, 2$, X_{Gi} is normally distributed with mean $A\epsilon_G b_G L/v$ and $\frac{\tan^{-1}\left(\frac{L}{2r}\right) A\epsilon_G S_G}{2\pi v r} + B_G$, respectively, and standard deviation k_G times the square root of the mean, allows for the determination of the threshold level s_G used by the vendor [4] and the noise factor k_G given in Table 1.

To solve for c_G, we note that field test results [2] state that there were 2256/162,958=0.014 false positives, which was defined as being 15% above background, and 50% of these alarms, or 0.007 of the tests, generated readings greater than 40% of background. Let C_G be a log-normal random variable with median e^{c_G} and dispersion $e^{\sigma_{cN}}$. We model the gamma-ray measurement X_G as a normal random variable with mean μ_G and standard deviation $k_G\sqrt{\mu_G}$, where $\mu_G = \frac{A\epsilon_G C_G L}{4\pi r^2 v} + B_G$, and derive c_G and σ_G by solving (with $b_G = 1400$ gamma rays/m^2·sec, $r = 2$ m and $L =$ 40 ft)

$$P\Big(X_G > \frac{1.15A\epsilon_G b_G L}{v}\Big) = 0.014, \tag{6}$$

$$P\Big(X_G > \frac{1.4A\epsilon_G b_G L}{v}\Big) = 0.007. \tag{7}$$

Passive gamma testing of the uranium weapon is done at the 1.001 MeV level, which has $\epsilon_G = 0.57$ and $b_G = 860$ gamma rays/m^2·sec [1]. To compute the source term for equations (4)-(5), we consider 1 kg of ^{235}U [4]. The emissions from weapons-grade uranium are due to a decay product of ^{238}U at 1.001 MeV [1] with decay rate 81/g·sec [5]. Since 5.5% of weapons-grade uranium is ^{238}U [1], we have $S_G = 0.055(1000)(81) = 4455$ gamma rays/sec. To find b_G, we calculate that 7.15% of the energy of background radiation is at 1.001 MeV [6] using a 10% energy resolution [1], so that the background radiation should contain 0.0143 μSv/hr at 1.001 MeV. Using the conversion factor of 1.0 μSv/hr = 6.53×10^5 gamma rays/m^2·sec in a NaI detector at 1.001 MeV [7, 8], we find that $b_G =$ 9338 gamma rays/m^2·sec. Using these parameter values, we re-solve (4)-(7) to get $k_G = 0.069$, $e^{c_G} = 1.62$ gamma rays/sec and $e^{\sigma_{cG}} = 43.56$.

A.3 Radiography

Active radiography involves detailed engineering issues related to filtering algorithms, contrast detail and spatial resolution that vary across companies, and developing a mathematical model of this complex process would be a daunting dask. Our objective is to develop a rather simple mathematical model of radiography that allows the detection probability to depend on the size and composition of the weapon and its shielding, and allows the model parameters to be readily estimated from industrial data. In our model, we assume that N_A gamma rays per cm^2 are emitted through one side of a sequence of J solid objects, where object $j = 1, \ldots, J$ is of thickness r_j and has mean free path of gamma rays μ_{jG}^{-1}. The probability of any particular gamma ray being detected on the other side of the sequence of objects is given by g_A, which is approximated by [1]

$$g_A = \prod_{j=1}^{J} e^{-\mu_{jG} r_j}. \tag{8}$$

Hence, if each gamma ray behaves independently, then the observed output X_A from gamma radiography, which is the number of rays detected from a cm^2 of cross-sectional area, is a binomial random variable with parameters N_A and g_A. Because g_A is typically small and we will aggregate over a large enough cross-sectional area to make the sum of the N_A's large, we approximate the random variable X_A by a Poisson random variable with parameter $N_A g_A$, which is both its mean and its variance.

We derive N_A by assuming that a gamma radiography machine can penetrate 16 cm of steel (SAIC claims that its various models of VACIS machines can penetrate between 9.5 and 16.5 cm [9]), which means that the aggregated machine measurements retain a signal-to-noise ratio of one if a standard $5 \times 10 \times 20$ cm lead brick is behind the steel. Consider two scenarios: in scenario 1, the lead brick is behind 16 cm of iron (the main element of steel), and hence $g_{A1} = e^{-5\mu_{lG} - 16\mu_{iG}}$ by (8), where $\mu_{lG}^{-1} = 1.544$ cm and $\mu_{iG}^{-1} = 2.424$ cm are the mean free paths of gamma rays in lead and iron, respectively [10]. The 200 aggregated measurements (the brick's cross-section is 200 cm^2) constitute a Poisson random variable X_{A1} with mean $200 N_A g_{A1}$, because the sum of Poisson

random variables is itself Poisson. In scenario 2, the lead is absent and $g_{A2} = e^{-16\mu_{iG}}$. The aggregated random variable is Poisson with mean $200N_A g_{A2}$. Now let $\Delta = X_{A2} - X_{A1}$ be the difference in the number of detected gamma rays between the two scenarios. Its mean is $200N_A(g_{A2} - g_{A1})$ and its standard deviation is $\sqrt{200N_A(g_{A1} + g_{A2})}$ because the two measurements are independent. Finally, we determine N_A so that the mean of Δ equals the standard deviation of Δ (this is what is meant by a signal-to-noise ratio of one), which yields

$$N_A = \frac{g_{A1} + g_{A2}}{200(g_{A2} - g_{A1})^2}. \tag{9}$$

A.4 False Positive Probabilities

We assume a fraction $f_T = 0.97$ of US-bound containers are trusted, meaning that they have not been flagged by the ATS. We view the testing system as having four stages: passive neutron monitoring (N), passive gamma monitoring (G), active radiography (A), and manual testing (M). For $i = \{N, G, A\}$, let f_i equal the false positive probability that a container generates an alarm for test i. Note that a weapon-free container can generate a false positive for three reasons: its contents, the natural background (in the case of passive testing), and measurement error.

The values of f_i are not set exogenously, but rather are determined by the test threshold parameters s_N, s_G and p_A, respectively, which are decision variables in our model. By the same reasoning as in (6), we have for $i = \{N, G\}$,

$$f_i = P\Big(X_i > s_i\Big), \tag{10}$$

where X_i is a normal random variable with mean μ_i and standard deviation $k_i\sqrt{\mu_i}$, where μ_i itself is the random variable $Z_i = \frac{A\epsilon_i C_i L}{4\pi r^2 v} + B_i$.

In contrast to passive testing, active testing can cause alarms for a variety of reasons that are independent of nuclear or radiological emissions. Consequently, we assume that $\tilde{f}_A = 0.05$ of actively tested containers set off an alarm regardless of the value of the threshold parameter

p_A, simply because an unexpected or mysterious object is seen [11]. In addition, an active testing alarm occurs if the container's contents are too dense for radiography to penetrate (e.g., shipments of metal objects, or certain agricultural shipments) or too difficult to decipher (e.g., the container contains a hodgepodge of items). Because containers filled with metal objects typically are 20 ft in length (to satisfy the weight limit), for modeling purposes we assume that a fraction $f_d = 0.1$ of containers are 20 ft in length and contain 24 cm of steel ($= 10\%$ packing fraction $\times$ 8 ft) along the direction measured by active testing. These containers are surrogates for all 20-ft and 40-ft dense or indecipherable containers, and the test threshold level p_A is applied only to these dense containers. By (8)-(9), each of these containers has a test measurement given by a Poisson random variable X_{An} with mean

$$g_{An} = e^{-\mu_{iG} r_n}, \tag{11}$$

where $\mu_{iG}^{-1} = 2.424$ cm (iron) and $r_n = 24$ cm. We assume that an alarm occurs if the probability that the radiography measurement equals zero, which is $e^{-N_A g_{An}}$, is greater than the threshold p_A. Hence, the total false positive probability takes on one of two values:

$$f_A = \begin{cases} \tilde{f}_A & \text{if} \quad e^{-N_A g_{An}} \leq p_A; \\ \tilde{f}_A + f_d & \text{if} \quad e^{-N_A g_{An}} > p_A. \end{cases} \tag{12}$$

If $p_A = 1$ then containers never fail radiography because of their denseness, whereas a value of p_A near 0 provides a more aggressive strategy against dense containers (i.e., these containers fail active testing and are subsequently opened up because they were too dense to penetrate).

A.5 Detection Probability

There are three layers of protection to detect a weaponized container before it enters the port of embarkation: C-TPAT's certification system, mechanical container seals and the ATS software system. Recall that the weapon can be hidden in a 40-ft or 20-ft container from a certified or uncertified shipper. Define d_C to be the probability that a certified shipper would catch a terrorist

attempting to smuggle a nuclear weapon in one of its containers, d_S to be the probability that the mechanical seal sets off an alarm if a terrorist inserts the nuclear weapon into the container, and d_E to be the probability that the software system ATS would detect a container from an uncertified shipper that contained a nuclear weapon.

For $i = \{N, G, A\}$, let d_i be the probability that test i would detect a nuclear weapon. These probabilities depend on the testing decisions s_N, s_G and p_A, and the shielding thickness r_s. We assume that the lithium hydride shielding reduces the neutron and gamma emissions by the multiplicative factors f_{sN} and f_{sG}, respectively; e.g., if the neutron emissions are reduced by a factor of 100 then $f_{sN} = 0.01$. Since the neutron detector aggregates the neutrons detected over all energy levels, we are interested in the fraction of neutrons emitted by the weapon that is not absorbed by the shielding. We approximate this fraction by $f_{sN} = e^{-\mu_{sN} r_s}$ [1, 12], where μ_{sN}^{-1} is the mean free path of neutron absorption in lithium hydride. We set $\mu_{sN}^{-1} = 3.13$ cm, using the observation that $r_s = 20$ cm reduces the neutron emissions of the plutonium weapon in Fetter et al. by a factor of 600 [1]. By (8), we assume that the fraction of gamma rays undegraded in energy is $f_{sG} = e^{-\mu_{sG} r_s}$, where $\mu_{sG}^{-1} = 10.725$ cm is the mean free path of gamma rays in lithium hydride at 0.662 MeV for the plutonium weapon and μ_{sG}^{-1}=13.02 cm is the mean free path of gamma rays in lithium hydride at 1.001 MeV for the uranium weapon [10]. For $i = \{N, G\}$, we have from (5) that

$$d_i = P\Big(X_i > s_i\Big), \tag{13}$$

where X_i is a normal random variable with mean μ_i and standard deviation $k_i\sqrt{\mu_i}$, where $\mu_i = \frac{f_{si}\tan^{-1}\left(\frac{L}{2r}\right)A\epsilon_i S_i}{2\pi v r} + B_i$.

To derive d_A, we define X_{Aw} by (8)-(9), where for the plutonium weapon,

$$g_{Aw} = e^{-(1.5\mu_{pG}+4\mu_{bG}+6\mu_{tG}+20\mu_{eG}+2\mu_{aG}+2\mu_{sG}r_s+\theta\mu_{iG}[244-42-2r_s])}, \tag{14}$$

where θ is the packing fraction; in equation (28), we change 1.5 cm to 2.46 cm, and 42 cm to 46 cm, for the uranium weapon (figure 2 of main text). To understand (14), note that the container,

which is 8 ft (or 244 cm) across, consists of the weapon (figure 2 of the main text), which is 42 cm in diameter and contains a 8.5 cm diameter empty core, a 1.5 cm thick layer (0.75 cm on each side of the weapon) of plutonium (with mean free path $\mu_{pG}^{-1} = 0.786$ cm; all mean free paths of gamma rays in (14) are at 1.3 MeV, which is the energy used in the newest VACIS machines [13], and are taken from [10]), 4 cm of beryllium (mean free path $\mu_{bG}^{-1} = 10.932$ cm), 6 cm of tungsten (mean free path μ_{tG}^{-1} =0.957 cm), 20 cm of high explosives (with mean free path $\mu_{eG}^{-1} = 9.185$ cm, calculated as in [14] from the composition of hydrogen, carbon, nitrogen and oxygen in the ratio 2:1:2:2 [1]), and 2 cm of aluminum (mean free path $\mu_{aG}^{-1} = 6.871$ cm), a layer of lithium hydride shielding of thickness r_s on both sides of the weapon ($\mu_{sG}^{-1} = 14.854$ cm), and a collection of identical iron objects ($\mu_{iG}^{-1} = 2.424$ cm) that have packing fraction θ. The packing fraction is given by

$$\theta = \frac{\left(2.95 \times 10^7 \text{ g} - \frac{4}{3}\pi[(r_s+21)^3 - 21^3] \text{ cm}^3 \ 1.2 \text{ g/cm}^3\right)/7.8 \text{ g/cm}^3}{[7.25 \times 10^7 - \frac{4}{3}\pi(r_s+21)^3] \text{ cm}^3} \quad \text{for a } 40-\text{ft container}, \tag{15}$$

$$\theta = \frac{\left(2.95 \times 10^7 \text{ g} - \frac{4}{3}\pi[(r_s+21)^3 - 21^3] \text{ cm}^3 \ 1.2 \text{ g/cm}^3\right)/7.8 \text{ g/cm}^3}{[3.62 \times 10^7 - \frac{4}{3}\pi(r_s+21)^3] \text{ cm}^3} \quad \text{for a } 20-\text{ft container}, \tag{16}$$

for the plutonium weapon; the 21 cm is changed to 23 cm in (15)-(16) for the uranium weapon (figure 2 of the main text). The numerator of (15) is the container weight limit (65k lbs) minus the weight of the lithium hydride shielding (assuming it is a concentric shell, where the density of the lithium hydride shielding is 1.2 g/cm^3 [1], which is about 50% higher than the density under normal conditions), divided by the density of steel; this ratio is the volume of steel that can be put into the container (ignoring the weight of the weapon, which is only 129 kg [1]). The denominator of (15) is the total container volume minus the volume of the shielded weapon. Equation (16) differs from (15) only in the calculation of the total container volume in the denominator.

There are two distinct portions of the container as it is scanned lengthwise: the weapon-

containing portion and the weapon-free portion. Because the outer radius of the tungsten layer is 10 cm [1] and the spatial resolution of gamma radiography is about 1 cm [9], we assume that radiography obtains $\pi 10^2 = 314$ weapon-containing measurements that are independent Poisson random variables with mean $N_A g_{Aw}$. The weapon-free portion of the container has $g_{An} = e^{-244\theta\mu_{iG}}$, since it is filled with identical iron objects according to the packing fraction θ. Because radiography generates nearly 3×10^5 weapon-free measurements from a 40-ft container, we can safely assume that g_{An} is correctly estimated during scanning. We allow the weapon to be detected via two approaches. First, as in (12), the container fails radiography if it is too dense, i.e., if $e^{-N_A g_{An}} > p_A$. Second, the weapon is detected if the 314 weapon-containing measurements differ significantly from the weapon-free measurements. For $j = \{n, w\}$, let $\tilde{X}_{Aj}$ be the sum of 314 independent samples from X_{Aj}, which itself is a Poisson random variable with mean $314 N_A g_{Aj}$. We assume that the weapon is detected if the aggregate measurement $\tilde{X}_{Aw}$ is less than the 0.05 tail of $\tilde{X}_{An}$; i.e., if the aggregate weapon measurement differs, at the 5% significance level, from the aggregate measurement we would expect to see from the weapon-free portion of the container. Taken together, we assume that

$$d_A = \begin{cases} 1 & \text{if} \quad e^{-N g_{An}} > p_A; \\ P(\tilde{X}_{Aw} < n^*) & \text{if} \quad e^{-N g_{An}} \leq p_A, \end{cases} \tag{17}$$

where

$$n^* = \min\left\{ n \;\middle|\; \sum_{k=0}^{n} \frac{(314 N_A g_{An})^k e^{-314 N_A g_{An}}}{k!} \geq 0.05 \right\}. \tag{18}$$

If the weapon is on a container of a certified shipper, then the detection probability (DP) for strategy YZ(a) is

$$\mathrm{DP}(\mathrm{YZ}(a)) = 1 - \prod_{i=\{C,S,N,G\}} (1 - d_i)(1 - a d_A) \quad \text{for Y} = \text{A, Z} = \text{E or D}, \tag{19}$$

$$\mathrm{DP}(\mathrm{YZ}(a)) = 1 - \prod_{i=\{C,S\}} (1 - d_i) \quad \text{for Y} = \text{U, Z} = \text{E or D}. \tag{20}$$

If the weapon is on a container of an uncertified shipper, then the detection probability is

$$\mathrm{DP}(\mathrm{YZ}(a)) = 1-(1-d_S)\Big[\prod_{i=\{E,N,G\}}(1-d_i)(1-ad_A)+d_E\prod_{i=\{N,G,A\}}(1-d_i)\Big] \text{ for } \mathrm{Y}=\mathrm{A},\ \mathrm{Z}=\mathrm{E} \text{ or } \mathrm{D}, \tag{21}$$

$$\mathrm{DP}(\mathrm{YZ}(a)) = 1-(1-d_S)\Big[(1-d_E)+d_E\prod_{i=\{N,G\}}(1-d_i)(1-ad_A)\Big] \text{ for } \mathrm{Y}=\mathrm{U},\ \mathrm{Z}=\mathrm{E} \text{ or } \mathrm{D}. \tag{22}$$

If inspection is carried out at both ports, then the analogs to (19)-(22), respectively, are

$$\mathrm{DP}(\mathrm{AB}(a)) = 1-\prod_{i=\{C,S\}}(1-d_i)\Big[\prod_{i=\{N,G\}}(1-d_i)(1-ad_A)\Big]^2 \text{ if certified}, \tag{23}$$

$$\mathrm{DP}(\mathrm{UB}(a)) = 1-\prod_{i=\{C,S\}}(1-d_i) \text{ if certified}, \tag{24}$$

$$\mathrm{DP}(\mathrm{AB}(a)) = 1-(1-d_S)\left[(1-d_E)\left(\prod_{i=\{N,G\}}(1-d_i)(1-ad_A)\right)^2+d_E\left(\prod_{i=\{N,G,A\}}(1-d_i)\right)^2\right] \text{ if uncertified}, \tag{25}$$

$$\mathrm{DP}(\mathrm{UB}(a)) = 1-(1-d_S)\left[(1-d_E)+d_E\left(\prod_{i=\{N,G\}}(1-d_i)(1-ad_A)\right)^2\right] \text{ if uncertified}. \tag{26}$$

B Congestion

The parametric-decomposition approach, which is used to estimate the probability distribution for the amount of time a container spends in the testing process at each port, is described in §B.1. The queueing networks at the port of embarkation and the port of debarkation are specified in §B.2 and §B.3, respectively. The values of the congestion parameters are given in Table 2. As explained in the main text, we ignore any congestion due to passive testing and we consider a single isolated ship that loads or unloads 3000 containers.

B.1 The Parametric-decomposition Approach

In the parametric-decomposition procedure [15], each queue in a network is characterized by five parameters: the arrival rate λ, the coefficient of variation (i.e., standard deviation divided by the

mean) of interarrival times c_a, the service rate μ for each server, the coefficient of variation of service times c_s, and the number of servers m.

In this subsection, we state the waiting time distribution at a generic queue with the five parameters given in the previous paragraph, as approximated by Whitt [15, 16]. In §B.2 and B.3, we derive four of the five parameters (the number of servers is a decision variable) for each of the queues in the testing networks, using subscripts to describe the port (E or D) and/or the test (A or M). The resulting waiting time distributions and service time distributions at each queue will then be combined to derive the total sojourn time distribution.

Let $\rho = \frac{\lambda}{m\mu}$ be the traffic intensity and $\beta = \sqrt{m}(1-\rho)$. We need to choose m so that $\rho < 1$ in order to maintain finite waiting times. Let W denote the steady-state waiting time in queue and D represent the conditional wait, given that the m servers are busy, i.e. $D = (W|W > 0)$. The expected waiting time in queue is approximated by

$$E(W) \approx \frac{c_a^2 + c_s^2}{2m\mu(1-\rho)(1+\sqrt{2\pi}\beta\Phi(\beta)e^{\beta^2/2})}, \tag{27}$$

where $\Phi(\cdot)$ is the cumulative distribution function of the standard normal, and

$$P(W > 0) \approx \min\left\{1, \frac{1-\Phi\Big(2\beta/(1+c_a^2)\Big)}{\Big(1-\Phi(\beta)\Big)(1+\sqrt{2\pi}\beta\Phi(\beta)e^{\beta^2/2})}\right\}. \tag{28}$$

Using (27)-(28), we approximate the expected value of D by

$$E(D) \approx \frac{E(W)}{P(W>0)}, \tag{29}$$

and approximate the squared coefficient of variation of D by

$$c_D^2 \approx 2\rho - 1 + \frac{4(1-\rho)(2c_s^2+1)}{3(c_s^2+1)}. \tag{30}$$

The distribution of W is approximated by a point mass at zero with probability $1 - P(W > 0)$ using (28), and fitting a probability density function to D using (29)-(30), according to one of four cases, as described in equations (55)-(61) of [15].

The parametric-decomposition procedure approximates c_a at a downstream queue in terms of c_d, which is the coefficient of variation of the departure process of the upstream queue, and the fraction of containers exiting the upstream queue that go to the downstream queue. By [15], c_d^2 at a queue is approximated by

$$c_d^2 \approx 1 + (1-\rho^2)(c_a^2 - 1) + \frac{\rho^2}{\sqrt{m}}(c_s^2 - 1), \tag{31}$$

and if the departure process is randomly thinned (in our case, via testing) with probability p, then the resulting squared coefficient of variation of the interarrival times at the downstream queue is approximated by

$$pc_d^2 + 1 - p. \tag{32}$$

B.2 Port of Embarkation

Testing is performed at the gates leading into the terminal at the port of embarkation. We assume that US-bound containers arrive to the port of embarkation according to a Poisson process at rate λ_E. These containers arrive according to an appointment system with a one-hour time window, and typically arrive 6-8 hours before being loaded. If each truck driver behaves independently within the constraints of the appointment system, then the Poisson assumption is reasonably accurate [17]. To estimate λ_E, consider a US-bound ship that will load 3000 containers at the port of embarkation (see figure 1)). With four ship cranes each performing 30 moves/hr, this vessel will take 25 hours to load. Suppose containers are scheduled to arrive at constant rate λ_E from time 0 to time τ_2 (i.e., $\lambda_E = 3000/\tau_2$) and suppose loading starts at time $\tau_1 > 0$ and ends at time $\tau_1 + 25$. If we ignore variability, set the maximum waiting time for any container at 8 hours (i.e., $\tau_1 + 25 - \tau_2 = 8$), and assume that, to avoid ship-crane idleness, two hours worth of work (i.e., 240 containers) is at the ship crane before it starts loading (i.e., $3000\tau_1/\tau_2 = 240$), then $\tau_1 = 1.48$ hr, $\tau_2 = 18.48$ hr, and $\lambda_E = 162.3$/hr.

The arrival rate to active testing is

$$\lambda_{EA} = \lambda_E\Big[1 - f_T(1-a)\prod_{i=\{N,G\}}(1-f_i)\Big] \text{ for Strategy A,} \tag{33}$$

$$\lambda_{EA} = \lambda_E(1-f_T)\Big[1 - (1-a)\prod_{i=\{N,G\}}(1-f_i)\Big] \text{ for Strategy U.} \tag{34}$$

We assume $c_{aEA} = 1$, since a randomly thinned (i.e., containers randomly chosen with probability λ_{EA}/λ_E) Poisson process is also a Poisson process. We also assume $\mu_A = 20$/hr (i.e., three minutes to test a container [9]). Because the scan time is deterministic and the analysis of the scan is random, we assume that the service time is an Erlang (order two) random variable with $c_{sA}^2 = 0.5$. By (31), the squared coefficient of variation of the departure process from this queue is approximated by

$$c_{dEA}^2 \approx 1 + (1-\rho_{EA}^2)(c_{aEA}^2 - 1) + \frac{\rho_{EA}^2}{\sqrt{m_{EA}}}(c_{sA}^2 - 1), \tag{35}$$

where there are m_{EA} servers and the traffic intensity is $\rho_{EA} = \frac{\lambda_{EA}}{m_{EA}\mu_A}$.

Additional congestion will also be incurred by those containers that require manual inspection. Containers that pass both passive tests are manually tested only if they fail active testing, which occurs with probability f_A in (12). In contrast, containers that fail at least one of the two passive tests proceed from active testing to manual testing with probability $\tilde{f}_A + f_d$, regardless of the value of p_A in (12). That is, we assume that the passive testing failure is successfully diagnosed by active testing with probability $1 - \tilde{f}_A - f_d$, and the failure is diagnosed during manual testing otherwise. We denote the arrival rate of containers to manual inspection by λ_{EM}, which is given by

$$\lambda_{EM} = \lambda_E[1 - \prod_{i=\{N,G\}}(1-f_i)](\tilde{f}_A + f_d) + \lambda_E \prod_{i=\{N,G\}}(1-f_i)[f_T a + 1 - f_T]f_A \text{ for Strategy A,} \tag{36}$$

$$\lambda_{EM} = \lambda_E(1-f_T)\Big\{[1 - \prod_{i=\{N,G\}}(1-f_i)](\tilde{f}_A + f_d) + \prod_{i=\{N,G\}}(1-f_i)af_A\Big\} \text{ for Strategy U.} \tag{37}$$

By (32), the squared coefficient of variation of the interarrival times to manual testing is approximated by

$$c_{aEM}^2 = \frac{\lambda_{EM}}{\lambda_{EA}} c_{dEA}^2 + 1 - \frac{\lambda_{EM}}{\lambda_{EA}}, \tag{38}$$

where c_{dEA}^2 is given in (35).

Manual inspection is typically performed in teams. It takes five inspectors about three hours to completely empty and repack a container, and considerably less to open the container and peer inside. We assume that the mean service time is one hour ($\mu_A = 1$/hr) and that each of the m_{EM} servers represents a team of five inspectors. We assume that these service times are exponential (and hence $c_{sM}^2 = 1$), so that the probability that a manually-tested container is entirely emptied is about $e^{-3} = 0.05$.

For $i = \{A, M\}$, let the waiting time and the service time for queue i be denoted by W_{Ei} and S_{Ei}, respectively. Then the sojourn time T_E is given by

$$T_E = \begin{cases} 0 & \text{with probability } 1 - \frac{\lambda_{EA}}{\lambda_E}; \\ W_{EA} + S_{EA} & \text{with probability } \frac{\lambda_{EA} - \lambda_{EM}}{\lambda_E}; \\ W_{EA} + S_{EA} + W_{EM} + S_{EM} & \text{with probability } \frac{\lambda_{EM}}{\lambda_E}. \end{cases} \tag{39}$$

Because the waiting times and service times are independent, and the waiting times at various queues are assumed to be independent (e.g., [18]), the probability distribution of the steady-state total sojourn time T_E in the queueing network is approximated by a mixture (according to the probabilities in (39)) of the convolution of the waiting time and service time distributions at each queue.

B.3 Port of Debarkation

At the port of debarkation, passive monitoring is undertaken when the containers are on bombcarts just after the containers are taken off the ship, and active and manual testing is performed while the containers are on utility trucks, which pick up the containers after the bombcarts deposit them in the shipyard. We assume that three ship cranes, each working at rate 30/hr, are used to unload the

vessel, generating a container arrival rate of $\lambda_D = 90$/hr. The ship cranes work two shifts per day, and hence the 3000 containers from the ship are unloaded in about 33 hours, i.e. two days. The arrival rate λ_{DA} to active testing is again given by equations (33)-(34), but with the subscript D in place of E. If we view the ship unloading process as three servers working at 100% utilization (i.e., $\rho = 1$) with deterministic service times (i.e., $c_s = 0$), then equations (31)-(32) imply that the interarrival times of containers to active testing has squared coefficient of variation approximated by

$$c_{aDA}^2 \approx \frac{\lambda_{DA}}{\lambda_D}\Big[1 - \frac{1}{\sqrt{3}}\Big] + 1 - \frac{\lambda_{DA}}{\lambda_D}. \tag{40}$$

The service rates and coefficients of variation of service times for both active and manual testing are the same as at the port of embarkation. The arrival parameters λ_{DM} and c_{aDM} and the sojourn time T_D are given exactly as in (35)-(39), with the subscript D in place of E throughout.

C Costs

The total annual global cost $K(\text{YZ}(a))$ of strategy YZ(a) is given by

$$K(\text{YE}(a)) = k_{EP} + v_{EA}m_{EA} + v_{EM}m_{EM} \quad \text{for Y} = \text{A or U}, \tag{41}$$

$$K(\text{YD}(a)) = k_{DP} + k_{DA} + v_{DA}m_{DA} + v_{DM}m_{DM} \quad \text{for Y} = \text{A or U}, \tag{42}$$

$$K(\text{YB}(a)) = k_{DA} + \sum_{i=\{E,D\}} k_{iP} + v_{iA}m_{iA} + v_{iM}m_{iM} \quad \text{for Y} = \text{A or U}, \tag{43}$$

where, for i =E or D, k_{iP} is the annual cost of passive testing, k_{DA} is the annual cost of active testing at the port of debarkation that is independent of the number of active testers, and v_{ij} is the annual global cost per server for $j = A$ for active testing and $j = M$ for manual testing. We ignore the costs of C-TPAT, mechanical container seals and ATS, since these activities are assumed to already be in place. These seven cost parameters (see Table 3 for the values of the components of these parameters) take into account equipment and labor, and are assessed by the annual salary plus 0.2/yr times the cost of equipment.

For Strategy YZ(a), the passive testing cost is independent of Y and a, and only depends on Z (i.e., on where passive testing is performed). The cost of a passive portal monitor is about \$80k [11]. We assume that one portal detector is required per terminal. The 30 largest US seaports accounted for 99.5% of the imported containers in 2002 [19], and they have about 50 terminals in total. About 40 overseas ports ship to Pier 400 at Long Beach, and 105 ports ship to New York/New Jersey; the overlap between these ports is about 20, and some of these 125 distinct ports use several terminals. Hence, we estimate that there are about 150 terminals at ports of embarkation. We assume that each passive detector requires two full-time employees to operate each 8-hour shift per day, and each employee earns \$75k per year (we assume overseas monitors are manned by US employees). Hence, our passive cost parameters are

$$k_{EP} = 150 \text{ terminals} \times \left[\frac{0.2}{\text{yr}}\Big(\frac{\$80\text{k}}{\text{terminal}}\Big) + \Big(6 \text{ workers} \times \frac{\$75\text{k}}{\text{worker} \cdot \text{yr}}\Big)\right] = \frac{\$69.9\text{M}}{\text{yr}}, \tag{44}$$

$$k_{DP} = 50 \text{ terminals} \times \left[\frac{0.2}{\text{yr}}\Big(\frac{\$80\text{k}}{\text{terminal}}\Big) + \Big(4 \text{ workers} \times \frac{\$75\text{k}}{\text{worker} \cdot \text{yr}}\Big)\right] = \frac{\$15.8\text{M}}{\text{yr}}. \tag{45}$$

The cost of an active portal monitor is about \$100k, although truck-mounted monitors are considerably more expensive [11]. We assume that an active tester requires three operators (each earning \$75k) per shift annually. Active testers scale with the number of ship cranes. Domestically, the Los Angeles/Long Beach ports have 135 ship cranes and handle 44% of imports, while Savannah has 13 cranes and handles 4.3% of the imports. Hence, we assume that the number of domestic ship cranes is approximately $\frac{135}{0.44} \approx \frac{13}{0.043} \approx 300$. We assumed three ship cranes were used at the port of debarkation in §B.3, and so we scale the number of active testers required at the port of debarkation up by a factor of 100 to estimate the domestic costs. The number of overseas-to-domestic ship cranes is assumed to be identical to the corresponding ratio for terminals, which is three. Hence, we scale the overseas active testers up by the factor of 300, which is three times the domestic scale-up factor of 100. The annual cost per active tester at the two ports are

$$v_{EA} = 300 \times \left[\frac{0.2}{\text{yr}}\Big(\frac{\$100\text{k}}{\text{tester}}\Big) + \Big(\frac{9 \text{ workers}}{\text{tester}} \times \frac{\$75\text{k}}{\text{worker} \cdot \text{yr}}\Big)\right] = \frac{\$208.5\text{M}}{\text{yr}}, \tag{46}$$

$$v_{DA} = 100 \times \left[\frac{0.2}{\text{yr}} \Big(\frac{\$100\text{k}}{\text{tester}} \Big) + \Big(\frac{6 \text{ workers}}{\text{tester}} \times \frac{\$75\text{k}}{\text{worker} \cdot \text{yr}} \Big) \right] = \frac{\$47\text{M}}{\text{yr}}. \tag{47}$$

There are also active testing costs at the port of debarkation that are independent of the number of active testers. By the discussion of the logistics at the port of debarkation in §B.3, all actively-tested railbound containers require three crane movements by the tophandlers, compared to the traditional approach where railbound containers only required one movement by the tophandlers. If we let $p_r = 0.4$ denote the fraction of imported containers that are railbound, then the ratio of additional tophandlers required divided by the traditional (i.e., pre-inspection) number of tophandlers is

$$\frac{2p_r \frac{\lambda_{DA}}{\lambda_D}}{p_r + 2(1 - p_r)}. \tag{48}$$

Similarly, in the absence of inspection, only truckbound containers traveled on a utility truck, but now actively-tested railbound containers also require a trip in a utility truck. Therefore, the ratio of additional utility trucks required divided by the pre-inspection number of utility trucks is

$$\frac{p_r \frac{\lambda_{DA}}{\lambda_D}}{1 - p_r}. \tag{49}$$

Given the 3.4 tophandlers and 16.9 utility trucks per ship crane at Pier 400, we assume the three cranes used at the port of debarkation required 10 tophandlers and 51 utility trucks in the absence of inspection. Moreover, tophandlers cost about $150k and utility trucks cost $20k, and we assume the salary for the drivers are $75k and $50k per shift, respectively.

Tophandlers and utility trucks also scale with the number of ship cranes, with factors of 100 domestically and 300 overseas. Hence, the cost factor k_{DA} is given by

$$\begin{aligned} k_{DA} &= 100 \times \left[10 \text{ tophandlers} \times \frac{2p_r \frac{\lambda_{DA}}{\lambda_D}}{2 - p_r} \left[\frac{0.2}{\text{yr}} \Big(\frac{\$150\text{k}}{\text{tophandler}} \Big) + \frac{2 \text{ workers}}{\text{tophandler}} \Big(\frac{\$75\text{k}}{\text{worker} \cdot \text{yr}} \Big) \right] \right. \\ &+ 100 \times \left[51 \text{ utility trucks} \times \frac{p_r \frac{\lambda_{DA}}{\lambda_D}}{1 - p_r} \left[\frac{0.2}{\text{yr}} \Big(\frac{\$20\text{k}}{\text{utility truck}} \Big) + \frac{2 \text{ workers}}{\text{utility truck}} \Big(\frac{\$50\text{k}}{\text{worker} \cdot \text{yr}} \Big) \right] \right] \\ &= \left(\frac{2p_r \frac{\lambda_{DA}}{\lambda_D}}{2 - p_r} \right) \frac{\$180\text{M}}{\text{yr}} + \left(\frac{p_r \frac{\lambda_{DA}}{\lambda_D}}{1 - p_r} \right) \frac{\$530.4\text{M}}{\text{yr}}. \end{aligned}$$

The parameter k_{DA} for Strategy YD(a) depends on Y and a via λ_{DA} in (33)-(34).

Each manual inspection team consists of five workers, each earning \$80k/yr. Since manual testers also scale with the number of cranes, we have

$$v_{EM} = 200 \times \left[\frac{3 \text{ teams}}{\text{tester}} \times \frac{\$400\text{k}}{\text{team} \cdot \text{yr}} \right] = \frac{\$360\text{M}}{\text{yr}}, \tag{50}$$

$$v_{DM} = 100 \times \left[\frac{2 \text{ teams}}{\text{tester}} \times \frac{\$400\text{k}}{\text{team} \cdot \text{yr}} \right] = \frac{\$80\text{M}}{\text{yr}}. \tag{51}$$

D Strategy Optimization and Evaluation

Each of the six classes of policies (AD,AE,AB,UD,UE,UB) contain six decision variables, which are listed in Table 4; we assume that these six variables take on the same value at each port in the three "B" policies. Hence, as noted in the main text, the US Government essentially has eight decisions: A or U; E, D, or B; and the six variables in Table 4. We evaluate each of these six classes of policies by choosing the decision variables to maximize the detection probability subject to a budget constraint of B dollars on the annual global cost, and congestion constraints at both ports. For the port of embarkation, we use the congestion constraint that at least 99% of containers make it through the testing process within 6 hours. This should lead to minimal impact on port efficiency and wreak little havoc on the loading plan. For the port of debarkation, we assume that at least 95% of containers make it through the testing process within 4 hours. Here, we are holding up individual containers and not an entire ship, and so we can use a lower service level.

The terrorists have three decisions: the shielding thickness r_s, a 20-ft or 40-ft container, and a certified or uncertified shipper. The optimization problem corresponding to the Stackelberg game [20], where the US Government makes its decisions before the terrorists, is

$$\max_{\{a,m_A,m_M,s_N,s_G,p_A\}} \quad \min_{\substack{r_s \\ \text{20-ft or 40-ft} \\ \text{certified or uncertified}}} \quad \text{DP}(\text{YZ}(a)) \tag{52}$$

$$\text{subject to} \quad K(\text{YZ}(a)) \leq B, \tag{53}$$

$$P(T_E > \ 6 \text{ hr}) \leq 0.01, \tag{54}$$

$$P(T_D > \ 4 \text{ hr}) \leq 0.05, \tag{55}$$

$$\frac{4}{3}\pi\bigg(\Big(r_s + 21\Big)^3 - 21^3\bigg)1.2 \leq 5.9 \times 10^6, \tag{56}$$

where DP(YZ(a)) is defined in (19)-(26), K(YZ(a)) is defined in (41)-(43), and T_E and T_D are defined in (39), where it is understood that, with probability one, $T_E = 0$ if $Z = D$ and $T_D = 0$ if $Z = E$. Constraint (56) (expressed in grams) is based on the assumption that the ATS would not detect the shielding as long as the weight of the lithium hydride shielding is no more than 13k lbs, which is 20% of the container weight limit (we omit the mass of the weapon, which is only 129 kg [1]). The left side of (56) assumes the shield is a concentric shell, and follows from (14); in (56), we change 21 cm to 23 cm for the uranium weapon (figure 2 of the main text). Constraint (56) reduces to $r_s \leq 84.8$ cm for the plutonium weapon; the corresponding outer radius of shielding is $84.8 + 21 =$105.8 cm, which is slightly less than the space constraint of 122 cm. By re-optimizing for different values of B in (53), we generate the cost vs. detection probability curves in the main text.

The initial input to the optimizer is a set of values for the decision variables a, s_N, s_G, p_A, from which we compute the minimum cost combination of m_A and m_M that will satisfy the maximum waiting time constraints (54)-(55). The optimizer then computes the numerical gradient of the objective function with the initial set of decision variable values. It uses the gradient to determine how it should alter the decision variables to produce the greatest increase to the objective function, attempting progressively smaller steps of the decision variables in that direction until it finds a new set of values that still satisfies all the constraints and increases the objective function. The optimizer stops once the gradient is too small (indicating that the function is barely changing) or when it can no longer find a new set of values that both satisfies the constraints and increases the objective function.

E Alternative Modes of Testing

In this section, we discuss alternative uses of existing technologies as well as technologies under development. The more promising options are considered in §8 of the main text.

E.1 Passive Testing at the Ports

Portal monitors are only one option for passive neutron and gamma testing at the ports of embarkation and debarkation. Handheld devices have considerably higher false positive probabilities and are much slower than portal monitors [2], making them impractical for front-line testing. However, they can be quite helpful in the investigation of containers that fail either passive or active testing.

Passive monitors can also be put on the ship cranes. One possibility is to put a sensor on the spreader bar that hovers over the container as it is handled. In this case, t is about 30 sec, r is about 1.5 m, and A_s and ϵ_s are similar to handheld devices. However, the results of an experiment in Norfolk, VA were not promising, due partly to the fluctuations in background radiation as the sensor moved in and out of the ship to get the container. Even if this serious technical issue can be overcome, another key hurdle is the durability of these monitors in such a harsh environment. Suppose the time between failures for a monitor on the beam is exponentially distributed with parameter τ (i.e, a mean of τ^{-1} hr). Because it is too expensive to stop the ship crane to fix the monitor during the crane's two shifts of operations at a port of debarkation, the monitor would be repaired during the third shift. Under this assumption, the fraction of time over the two shifts that the monitor is operating is given by $\frac{1-e^{-16\tau}}{16\tau}$. Hence, the detection probability and the false positive probability are both decreased by this factor.

A more promising option is to put the detector on the scaffold of the ship crane. In this case, t will be shorter (perhaps 5 sec), and A, ϵ_N and ϵ_G would be similar to the values in §A.1-§A.2 for a portal monitor. The monitor's reliability would be higher (i.e., smaller τ, because the scaffold undergoes less stress than the spreader bar) and its false positive rate would be lower (less

background fluctuations). However, given that passive portal monitoring does not significantly impact port congestion, there does not appear to be a compelling need to pursue these difficult options.

E.2 Elongated Portal Passive Testing

Rather than driving through the portal monitor at velocity v, we assume that a container takes 10 sec to drive into the portal and then stays there for t sec, generating emissions at the detector of $\frac{f_{si}A\epsilon_i S_i t}{4\pi r^2}$. We create a 3-stage queueing network by adding a queue in front of the two-stage network in §B.3. The Poisson arrival rate to this queue is $\lambda_E = 162.3$/hr, the service times are deterministic with duration $\mu_p^{-1} = 10 + t$ sec, and there are m_{EP} servers. There are two additional decision variables, the testing time (t) and the number of servers (m_{EP}). Because the testing process is highly automated, we assume that two workers can run this operation, regardless of the number of machines.

E.3 Passive Testing inside Containers

Passive monitors can also be put inside containers. Given the low false positive probability of passive neutron testing, these sensors might be able to exploit the week-long trip to improve the signal-to-noise ratio of passive neutron testing at the port of debarkation. The steel container walls, which are $r_c = 0.2$ cm thick, reduce the background neutron source at the detector by the factor $e^{-\mu_{iN} r_c}$, where $\mu_{iN}^{-1} = x$ cm is the mean free path of neutrons in steel. Hence, the true cumulative background emissions is a normal random variable B_N with mean $A\epsilon_N b_N t$ and standard deviation $\sqrt{A\epsilon_N b_N t}$, where $A = 0.02$ and $\epsilon_N = 0.05$ (similar to handheld devices [1]) and $t = 7$ days. The true weapon emissions at the detector would be $\frac{A\epsilon_N e^{-\mu_{iN} r_c} S_N t}{4\pi r^2}$, where $r = 1.2$ m (the halfwidth of a container). The remainder of the model remains unchanged, including the assumption that the typical weaponless container has no neutron emissions (i.e., $C_N = 0$ with probability one). Note

that containers far from direct sunlight may receive a smaller background radiation rate than b_N, which causes us to underestimate the efficacy of this option. The cost of each sensor is assumed to be \$50, and the 0.2/yr equipment factor is applied.

E.4 X-ray Radiography

X-ray radiography is capable of penetrating up to 41 cm of steel [21]. However, this increased penetration is achieved with a 9-MeV x-ray source, which requires considerable safety precautions. Consequently, it is practical to only use these \$1.2M machines for containers that cannot be penetrated by gamma radiography. We consider a strategy where all dense containers that are actively tested are routed to x-ray radiography, and all other actively tested containers are routed to gamma radiography. We further assume that the fraction $\tilde{f}_A$ of containers that cause false positives are all processed by gamma radiography. If we assume that the service time characteristics of gamma radiography are the same as x-ray radiography and denote the service time and waiting time at x-ray radiography at the embarkation port by S_{EX} and W_{EX}, respectively, then equation (19) is replaced by

$$T_E = \begin{cases} 0 & \text{with probability } 1 - \frac{\lambda_{EA}}{\lambda_E}; \\ W_{EA} + S_{EA} & \text{with probability } \frac{(1-f_d-\tilde{f}_A)\lambda_{EA}}{\lambda_E}; \\ W_{EX} + S_{EX} & \text{with probability } \frac{f_d\lambda_{EA}}{\lambda_E}; \\ W_{EA} + S_{EA} + W_{EM} + S_{EM} & \text{with probability } \frac{\tilde{f}_A\lambda_{EA}}{\lambda_E}. \end{cases} \tag{57}$$

To estimate how the x-ray equipment would perform, we replace 16 cm by 41 cm in g_{A1} and g_{A2} in equation (9) and calculate a new value of N_A. In this and all other calculations to find the false positive probability and detection probability for active testing, we use the following mean free paths at 9MeV: lithium hydride (45.0 cm), beryllium (31.6 cm), explosives (24.4 cm), aluminum (15.6 cm), iron (4.26 cm), lead (1.83 cm), tungsten (1.13 cm), plutonium (0.974 cm).

E.5 Networked Active Testing

Active testing throughput can be increased by electronically transmitting the scanned images and allowing multiple scans to be analyzed simultaneously, thereby decoupling scan production and scan analysis. To analyze the congestion resulting from this option, we consider a 3-stage queueing network consisting of scan production ($\mathrm{A_p}$), scan analysis ($\mathrm{A_a}$), and manual testing (M). The arrival parameters λ_{EA_p}, $c^2_{aEA_p}$, λ_{DA_p} and $c^2_{aDA_p}$ are identical to λ_{EA}, c^2_{aEA}, λ_{DA} and c^2_{aDA} respectively, in §B.2 and §B.3. The service rate at the scan production queue is $\mu_{A_p} = 60$/hr and the service times are assumed to be deterministic ($c_{sA_p} = 0$). Since all scans are analyzed, $\lambda_{iA_a} = \lambda_{iA_p}$ for $i =$E or D, and equations (31)-(32) imply that

$$c^2_{aiA_a} \approx 1 + (1 - \rho^2_{iA_p})(c^2_{aiA_p} - 1) - \frac{\rho^2_{iA_p}}{\sqrt{m_{iA_p}}} \quad \text{for} \quad \mathrm{i = E \text{ or } D}. \tag{58}$$

We assume that $\mu_A = 30$/hr, so that the mean total active testing time is the same as in the base case (i.e., $\mu_A^{-1} = \mu_{A_p}^{-1} + \mu_{A_a}^{-1}$). Similarly, we assume $c^2_{sA_a} = \frac{9}{8}$ (for simplicity, S_{iA_a} in (60) is assumed to be exponential), so that the squared coefficient of variation of the total testing time is the same as in the base case (i.e., $c^2_{sA_a} = \frac{\mu^2_{A_a}}{\mu^2_A} c^2_{sA}$). The arrival rates to manual inspection, λ_{EM} and λ_{DM}, are given by (36)-(37), and

$$c^2_{aiM} \approx \frac{\lambda_{iM}}{\lambda_{iA_p}} c^2_{diA_a} + 1 - \frac{\lambda_{iM}}{\lambda_{iA_p}} \quad \text{for} \quad \mathrm{i = E \text{ or } D}. \tag{59}$$

The service parameters μ_M and c_{sM} of manual testing are the same as in the base case. The total sojourn time is given by, for $i =$E or D,

$$T_i = \begin{cases} 0 & \text{with probability } 1 - \frac{\lambda_{iA_p}}{\lambda_i}; \\ W_{iA_p} + S_{iA_p} + W_{iA_a} + S_{iA_a} & \text{with probability } \frac{\lambda_{iA_p} - \lambda_{iM}}{\lambda_i}; \\ W_{iA_p} + S_{iA_p} + W_{iA_a} + S_{iA_a} + W_{iM} + S_{iM} & \text{with probability } \frac{\lambda_{iM}}{\lambda_i}. \end{cases} \tag{60}$$

We assume that each of the servers at scan production consist of an active tester ($100k each) and two operators ($75k/yr each), and each server at scan analysis consists of one inspector ($75k/yr each).

F Radiological

There are seven important radioisotopes [22] that can be put into radiological dispersal devices (RDDs), or so-called dirty bombs: ^{241}Am (found in smoke detectors), ^{252}Cf, ^{137}Cs (spent nuclear fuel and brachytherapy), ^{60}Co (nuclear reactors, food radiation), ^{192}Ir (cameras), ^{238}Pu (thermal generators), and ^{90}Sr (nuclear waste, television tubes). There are three main kinds of ionizing radiation: alpha particles, which only travel 4 cm but are harmful if inhaled; beta particles, which travel 2 m and can cause skin burns; and gamma rays and x-rays, which pose serious risks. ^{241}Am, ^{252}Cf and ^{238}Pu only emit alpha particles, and so can be easily handled by terrorists, whereas the other four isotopes can be fatal if handled in sufficient quantities.

Levi [22, 23] estimates that 2 Ci of ^{137}Cs (an amount found in many medical gauges) in 10 pounds of TNT would cause a km^2 (40 city blocks) to exceed EPA radiological standards, whereas a Russian study [24] states that between 50 and 10k Ci of ^{137}Cs in 50 kg of TNT could cause the population in a 1 km^2 area to seek shelter. The discrepancy between these studies could be due to the different safety thresholds used, the fact that the population in the Russian analysis takes protective measures, different amounts of explosives, and different atmospheric models (the Russian model is more complex). For concreteness, we consider a radiological source of 10 Ci (0.11 g) of ^{137}Cs.

Unlike fissile material, the emissions from dirty bomb materials are not due to the fission process. Consequently, radioactive material will be detected by its emitted gamma rays. Ten Ci of ^{137}Cs, if unshielded, generates 3.6×10^{12} gamma rays/sec, of which 46.92% is at 0.662 meV. Hence, the peak gamma-ray emission rate is 1.69×10^{12} rays/sec, compared with 600 or 30 gamma rays/sec for the nuclear sources considered in the main text. To reduce the radiological gamma-ray emissions to the mean plus 3 standard deviations of the background, $A\epsilon_G b_G L/v + 3\sqrt{A\epsilon_G b_G L/v}$, requires 8.23 cm of tungsten shielding. The corresponding g_{Aw} term in (14) is $e^{-16.46\mu_{tG}} = 3.4 \times 10^{-8}$, which is about 3 logs smaller than the g_{An} term in (17)-(18) for a 20-ft container, and about

5 logs smaller for a 40-ft container. Consequently, 10 Ci of ^{137}Cs is at least as easy to detect as a nuclear weapon: if enough shielding is used to hide the gamma-ray emissions, then gamma radiography will detect the radiological source if the surrounding steel items can be penetrated.

G Supplementary Computational Results

Tables 5-8 provides the detailed solutions for the points on the base-case curves in Figs. 4a-4d, respectively, of the main text.

References

[1] S. Fetter, V. A. Frolov, M. Miller, R. Mozley, O. F. Prilutsky, S. N. Rodionov, R. Z. Sagdeev, *Science & Global Security* **1**, 225 (1990).

[2] P. Beck, Paper OEFZS-G-0005, Austrian Research Centers, Seibersdorf (2000).

[3] E. F. Plechaty, J. R. Kimlinger, UCRL-50400, Vol. 14, Lawrence Livermore National Laboratory (July 4, 1976).

[4] http://www.tsasystems.com/products/portals/vm-250.php.

[5] S. Fetter, T. B. Cochran, L. Grodzins, H. L. Lynch, M. S. Zucker, *Science* **248**, 828 (1990).

[6] http://www.csupomona.edu/˜pbsiegel/www/nuclear.html.

[7] http://www.eas.asu.edu/holbert/eee460/HealthPhysics.pdf.

[8] http://physics.nist.gov/PhysRefData/XrayMassCoef/cover.html.

[9] R. D. Richardson, V. V. Verbinski, V. J. Orphan, *Port Technology Int'l.*, 83 (March 4, 2002).

[10] http://physics.nist.gov/PhysRefData/Xcom/Text/XCOM.html.

[11] S. Schiesel, *N.Y. Times*, Section E, p. 1 (March 20, 2003).

[12] R. L. Maughan, M. Yudelev, J. D. Forman, S. B. Williams, D. Gries, T. M. Fletcher, W. Chapman, E. J. Blosser, T. Horste, *Med. Phys.* **28**, 1006 (2001).

[13] M. P. Snell, *Port Technology Int'l.*, 83 (date).

[14] http://www.tpub.com/doenuclearphys/nuclearphysics40.htm.

[15] W. Whitt, *Bell System Tech. J.* **62**, 2779 (1983).

[16] W. Whitt, *Production Operations Mgmt.* **2**, 114 (1993).

[17] E. Cinlar, in P. A. W. Lewis, Ed., *Stochastic Point Processes: Statistical Analysis, Theory and Applications*, Wiley, NY (1972).

[18] J. M. Harrison, V. Nguyen, *Queueing Systems* **6**, 1 (1990).

[19] http://www.aapa-ports.org/industryinfo/statistics.htm.

[20] R. Gibbons, *Game Theory for Applied Economists*, Princeton University Press, Princeton, NJ (1992).

[21] http://www.heimanncargovision.com/shockedpage.html.

[22] C. D. Ferguson, T. Kazi, J. Perera, Paper No. 11, Center for Nonproliferation Studies, Monterey Institute of International Studies (2003).

[23] M. A. Levi, H. C. Kelly, *Scientific American* 76 (Nov. 2002).

[24] L. Bolshov, R. Arutyunyan, O. Pavlovsky, *High-Impact Terrorism: Proceedings of a Russian-American Workshop*, pg 137, National Academy of Sciences (2002).

Parameter	Description	Value	Reference
L	Container length	20 or 40 ft	See text
v	Velocity during passive testing	2.2 m/sec	See text
A	Area of radiation detector	0.3 m^2	[1]
r	Distance of radiation detector	2 m	[2]
S_N	Neutron source	400k neutrons/sec	[1]
ϵ_N	Efficiency of neutron detector	0.14	[1]
b_N	Mean neutron background rate	50 neutrons/m^2·sec	[1]
e^{c_N}	Median container neutron emissions	0	[2]
$e^{\sigma_{cN}}$	Dispersion of container neutron emissions	1	[2]
k_N	Neutron noise factor	2.81	(2)-(3)
S_G	Gamma source	600 gamma rays/sec	[1]
ϵ_G	Efficiency of gamma detector	0.70	[1]
b_G	Mean gamma background rate	1400 gamma rays/m^2·sec	[1]
e^{c_G}	Median container gamma emissions	2.63 gamma rays/sec	(6)-(7)
$e^{\sigma_{cG}}$	Dispersion of container gamma emissions	43.63	(6)-(7)
k_G	Gamma noise factor	0.146	(4)-(5)
N_A	Effective radiography emissions	4.14 gamma rays/cm^2	(8)-(9)
f_T	Fraction of trusted containers	0.97	See text
$\tilde{f}_A$	Fraction of containers alarming active test	0.05	[11]
f_d	Fraction of dense containers	0.1	(12)
r_n	Thickness of metal in dense containers	24 cm	See text
d_C	Detection probability of certification	0.2	See text
d_S	Detection probability of seals	0.05	See text
d_E	Detection probability of ATS	0.05	See text

Table 1: Values for detection-modeling parameters.

Parameter	Description	Value	Reference
λ_E	Embarkation truck arrival rate	162/hr	See text
c_{aEA}	cv of interarrival times at embarkation, active test	1	See text
μ_A	Active testing rate	20/hr	[9]
c_{sA}	Coefficient of variation (cv) of active test times	$\sqrt{0.5}$	See text
μ_M	Manual testing rate	1/hr	See text
c_{sM}	Coefficient of variation (cv) of manual test times	1	See text
λ_D	Debarkation truck arrival rate	90/hr	See text

Table 2: Values for congestion parameters. All other congestion parameter values are derived from other parameters and decision variables.

Description	Value	Reference
Fraction of railbound containers (p_r)	0.4	See text
Number of US terminals	50	[19]
Number of overseas terminals	150	See text
Cost of passive tester	\$80k	[11]
Number of employees per passive tester	2	See text
Employee salary at active testing	\$75k/yr	See text
Cost of gamma radiography machine	\$100k	[11]
Number of employees per active tester	3	See text
Employee salary at active testing	\$75k/yr	See text
Cost of tophandler	\$150k	See text
Salary of tophandler operator	\$75k/yr	See text
Cost of utility truck	\$20k	See text
Salary of utility-truck driver	\$50k/yr	See text
Salary of manual tester	\$75k/yr	See text
Cost of passive monitor on a seal	\$50	See text
Cost of electronic tamper-resistant seal	\$100	See text
Number of containers worldwide	12M	See text
Cost of x-ray radiography machine	\$1.2M	See text

Table 3: Cost parameters.

Parameter	Description
a	Fraction active testing
s_N	Neutron threshold level
s_G	Gamma threshold level
p_A	Radiography threshold probability
m_A	Number of active testers
m_M	Number of manual testing teams

Table 4: Decision variables.

L	Cert.	Strat.	DP	Budget	Cost	d_N	d_A	a	m_{EA}	m_{EM}	m_{DA}	m_{DM}
20	U	EA	0.108	650	638	0.00	1.0	0.01	1	1	0	0
20	U	EA	0.108	800	638	0.00	1.0	0.01	1	1	0	0
20	U	EA	0.145	1000	998	0.00	1.0	0.05	1	2	0	0
20	U	EA	0.145	1200	998	0.00	1.0	0.05	1	2	0	0
20	U	EA	0.179	1500	1358	0.00	1.0	0.09	1	3	0	0
20	U	EA	0.216	2000	1927	0.00	1.0	0.13	2	4	0	0
20	U	EA	0.289	3000	2855	0.00	1.0	0.21	3	6	0	0
20	U	EA	0.399	4000	3935	0.00	1.0	0.33	3	9	0	0
20	U	EA	0.475	5000	4864	0.00	1.0	0.42	4	11	0	0
20	U	DA	0.106	160	160	0.00	1.0	0.01	0	0	1	1
20	U	DA	0.138	240	176	0.00	1.0	0.05	0	0	1	1
20	U	DA	0.207	320	289	0.00	1.0	0.12	0	0	1	2
20	U	DA	0.276	480	448	0.00	1.0	0.20	0	0	2	3
20	U	DA	0.345	640	561	0.00	1.0	0.27	0	0	2	4
20	U	DA	0.474	800	783	0.00	1.0	0.42	0	0	2	6
20	U	DA	0.542	1000	989	0.00	1.0	0.49	0	0	4	7
20	U	DA	0.807	1500	1482	0.00	1.0	0.79	0	0	5	11
20	U	DA	1.000	2000	1814	0.00	1.0	1.00	0	0	5	14
20	U	BA	0.118	800	799	0.00	1.0	0.01	1	1	1	1
20	U	BA	0.118	1000	799	0.00	1.0	0.01	1	1	1	1
20	U	BA	0.178	1250	1174	0.00	1.0	0.05	1	2	1	1
20	U	BA	0.189	1500	1257	0.00	1.0	0.05	1	2	1	2
20	U	BA	0.253	1750	1633	0.00	1.0	0.09	1	3	1	2
20	U	BA	0.259	2000	1995	0.00	1.0	0.09	1	4	1	2
20	U	BA	0.380	3000	2885	0.00	1.0	0.17	3	5	1	3
20	U	BA	0.496	4000	3767	0.00	1.0	0.25	3	7	2	4
20	U	BA	0.615	5000	4968	0.00	1.0	0.35	3	10	2	5

Table 5: Solutions corresponding to points in Fig. 4a of main text. Under Cert. column, C is uncertified and U is certified. We report d_N and d_A in lieu of s_N and p_A. For all scenarios, $d_G = 0.00$ and $r_s = 84.8$ cm. Cost and Budget figures are in millions of dollars.

L	Cert.	Strat.	DP	Budget	Cost	d_N	d_A	a	m_{EA}	m_{EM}	m_{DA}	m_{DM}
20	C	EA	0.264	650	638	0.03	1.0	0.00	1	1	0	0
20	C	EA	0.264	800	638	0.03	1.0	0.00	1	1	0	0
20	C	EA	0.280	1000	998	0.00	1.0	0.05	1	2	0	0
20	C	EA	0.280	1200	998	0.00	1.0	0.05	1	2	0	0
20	C	EA	0.309	1500	1358	0.00	1.0	0.09	1	3	0	0
20	C	EA	0.340	2000	1927	0.00	1.0	0.13	2	4	0	0
20	C	EA	0.401	3000	2855	0.00	1.0	0.21	3	6	0	0
20	C	EA	0.494	4000	3935	0.00	1.0	0.33	3	9	0	0
20	C	EA	0.558	5000	4864	0.00	1.0	0.42	4	11	0	0
20	C	DA	0.247	160	160	0.00	1.0	0.01	0	0	1	1
20	C	DA	0.275	240	176	0.00	1.0	0.05	0	0	1	1
20	C	DA	0.333	320	289	0.00	1.0	0.12	0	0	1	2
20	C	DA	0.391	480	448	0.00	1.0	0.20	0	0	2	3
20	C	DA	0.449	640	561	0.00	1.0	0.27	0	0	2	4
20	C	DA	0.557	800	783	0.00	1.0	0.42	0	0	2	6
20	C	DA	0.614	1000	989	0.00	1.0	0.49	0	0	4	7
20	C	DA	0.837	1500	1482	0.00	1.0	0.79	0	0	5	11
20	C	DA	1.000	2000	1814	0.00	1.0	1.00	0	0	5	14
20	C	BA	0.259	800	800	0.01	1.0	0.00	1	1	1	1
20	C	BA	0.287	1000	808	0.03	1.0	0.00	1	1	1	1
20	C	BA	0.335	1250	1182	0.06	1.0	0.00	1	2	1	1
20	C	BA	0.344	1500	1474	0.07	1.0	0.00	2	2	1	2
20	C	BA	0.376	1750	1635	0.09	1.0	0.00	1	3	1	2
20	C	BA	0.397	2000	1850	0.11	1.0	0.00	2	3	1	2
20	C	BA	0.499	3000	2892	0.19	1.0	0.00	3	5	1	3
20	C	BA	0.593	4000	3774	0.27	1.0	0.00	3	7	2	4
20	C	BA	0.677	5000	4817	0.35	1.0	0.00	4	9	2	5

Table 6: Solutions corresponding to points in Fig. 4b of main text. Under Cert. column, C is uncertified and U is certified. We report d_N and d_A in lieu of s_N and p_A. For all scenarios, $d_G = 0.00$ and $r_s = 84.8$ cm. Cost and Budget figures are in millions of dollars.

L	Cert.	Strat.	DP	Budget	Cost	d_N	d_A	a	m_{EA}	m_{EM}	m_{DA}	m_{DM}
40	U	EA	0.182	650	638	0.00	1.0	0.09	1	1	0	0
40	U	EA	0.182	800	638	0.00	1.0	0.09	1	1	0	0
40	U	EA	0.184	1000	846	0.00	1.0	0.10	2	1	0	0
40	U	EA	0.184	1200	846	0.00	1.0	0.10	2	1	0	0
40	U	EA	0.294	1500	1415	0.00	1.0	0.22	3	2	0	0
40	U	EA	0.296	1600	1566	0.00	1.0	0.22	2	3	0	0
40	U	EA	0.400	2000	1983	0.00	1.0	0.34	4	3	0	0
40	U	EA	0.616	3000	2912	0.00	1.0	0.57	5	5	0	0
40	U	EA	0.754	4000	3840	0.00	1.0	0.73	6	7	0	0
40	U	EA	0.983	5000	4977	0.00	1.0	0.98	8	9	0	0
40	U	DA	0.106	160	159	0.00	1.0	0.01	0	0	1	1
40	U	DA	0.273	240	239	0.00	1.0	0.19	0	0	1	1
40	U	DA	0.276	320	288	0.00	1.0	0.20	0	0	2	1
40	U	DA	0.479	480	464	0.00	1.0	0.42	0	0	2	2
40	U	DA	0.580	640	639	0.00	1.0	0.53	0	0	3	3
40	U	DA	0.690	800	739	0.00	1.0	0.66	0	0	4	3
40	U	DA	0.897	1000	965	0.00	1.0	0.89	0	0	5	4
40	U	DA	1.000	1500	1094	0.00	1.0	1.00	0	0	5	5
40	U	BA	0.120	800	799	0.00	1.0	0.01	1	1	1	1
40	U	BA	0.263	1200	1044	0.00	1.0	0.10	2	1	1	1
40	U	BA	0.447	1600	1583	0.00	1.0	0.22	2	2	2	2
40	U	BA	0.452	2000	1944	0.00	1.0	0.22	2	3	2	2
40	U	BA	0.731	3000	2949	0.00	1.0	0.45	4	4	3	3
40	U	BA	0.856	4000	3940	0.00	1.0	0.60	5	6	3	3
40	U	BA	0.971	5000	4939	0.00	1.0	0.82	7	7	4	4

Table 7: Solutions corresponding to points in Fig. 4c of main text. Under Cert. column, C is uncertified and U is certified. We report d_N and d_A in lieu of s_N and p_A. For all scenarios, $d_G = 0.00$ and $r_s = 84.8$ cm. Cost and Budget figures are in millions of dollars.

L	Cert.	Strat.	DP	Budget	Cost	d_N	d_A	a	m_{EA}	m_{EM}	m_{DA}	m_{DM}
40	C	EA	0.311	650	638	0.00	1.0	0.09	1	1	0	0
40	C	EA	0.311	800	638	0.00	1.0	0.09	1	1	0	0
40	C	EA	0.313	1000	846	0.00	1.0	0.10	2	1	0	0
40	C	EA	0.313	1200	846	0.00	1.0	0.10	2	1	0	0
40	C	EA	0.406	1500	1415	0.00	1.0	0.22	3	2	0	0
40	C	EA	0.408	1600	1566	0.00	1.0	0.22	2	3	0	0
40	C	EA	0.495	2000	1983	0.00	1.0	0.34	4	3	0	0
40	C	EA	0.677	3000	2912	0.00	1.0	0.57	5	5	0	0
40	C	EA	0.793	4000	3840	0.00	1.0	0.73	6	7	0	0
40	C	EA	0.986	5000	4977	0.00	1.0	0.98	8	9	0	0
40	C	DA	0.247	160	159	0.00	1.0	0.01	0	0	1	1
40	C	DA	0.388	240	239	0.00	1.0	0.19	0	0	1	1
40	C	DA	0.391	320	288	0.00	1.0	0.20	0	0	2	1
40	C	DA	0.561	480	464	0.00	1.0	0.42	0	0	2	2
40	C	DA	0.646	640	639	0.00	1.0	0.53	0	0	3	3
40	C	DA	0.739	800	739	0.00	1.0	0.66	0	0	4	3
40	C	DA	0.913	1000	965	0.00	1.0	0.89	0	0	5	4
40	C	DA	1.000	1500	1094	0.00	1.0	1.00	0	0	5	5
40	C	BA	0.259	800	799	0.00	1.0	0.01	1	1	1	1
40	C	BA	0.379	1200	1044	0.00	1.0	0.10	2	1	1	1
40	C	BA	0.534	1600	1583	0.00	1.0	0.22	2	2	2	2
40	C	BA	0.538	2000	1944	0.00	1.0	0.22	2	3	2	2
40	C	BA	0.773	3000	2949	0.00	1.0	0.45	4	4	3	3
40	C	BA	0.879	4000	3940	0.00	1.0	0.60	5	6	3	3
40	C	BA	0.975	5000	4939	0.00	1.0	0.82	7	7	4	4

Table 8: Solutions corresponding to points in Fig. 4d of main text. Under Cert. column, C is uncertified and U is certified. We report d_N and d_A in lieu of s_N and p_A. For all scenarios, $d_G = 0.00$ and $r_s = 84.8$ cm. Cost and Budget figures are in millions of dollars.

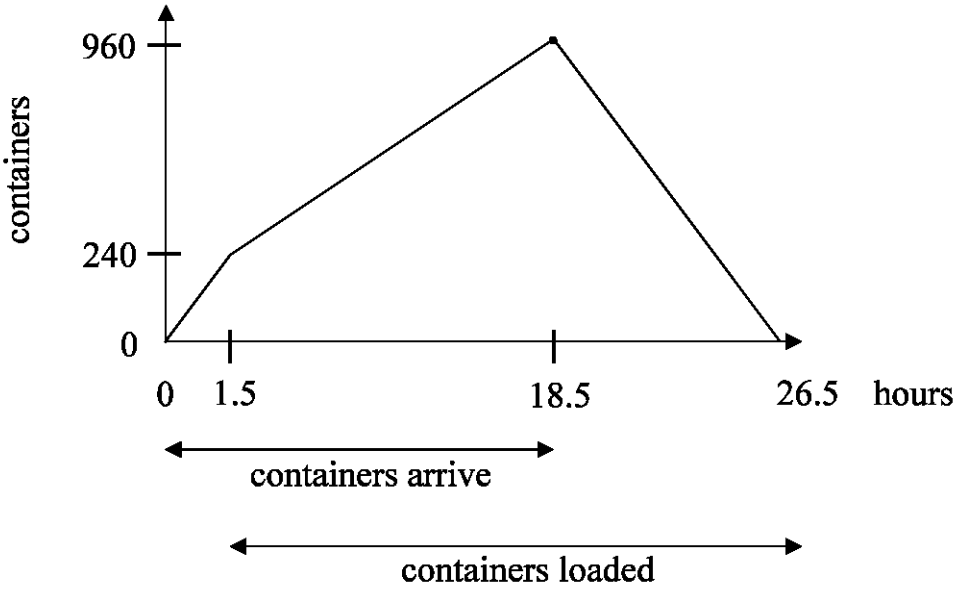

Figure 1: The derivation of λ_E in §B.2.